J Seismol (2007) 11:405–414
DOI 10.1007/s10950-007-9060-4

ORIGINAL ARTICLE

Shear wave velocity and crustal thickness in the Pannonian Basin from receiver function inversions at four permanent stations in Hungary

György Hetényi · Zoltán Bus

Received: 21 February 2007 / Accepted: 29 June 2007 / Published online: 1 August 2007

Abstract Receiver functions of teleseismic waveforms recorded at four Hungarian permanent broadband stations have been analyzed using semilinearized and stochastic inversion methods to estimate the crustal thickness and S wave velocity structure in the Pannonian Basin. The results of both inversion methods agree well with the crustal thicknesses obtained by previous seismic refraction and reflection studies in the regions which are densely covered with seismic lines (28 and 27 km in westernmost and southern Hungary, respectively) and suggest a thicker crust compared to what was known before beneath the Transdanubian and Northern Ranges (34 and 33 km, respectively). The comparison of the one-dimensional shear wave velocity models derived by the different inversion methods shows that, in case of simple, smoothly varying structures, the results do not differ significantly and can be regarded as absolute velocities. Otherwise, the recovered velocity gradients agree, but there are differences in the absolute velocity values. The back-azimuthal variations of both radial and tangential receiver functions are interpreted as dipping structure and as waves sampling different geological areas. The signature of the deep structure on low-frequency receiver functions suggests a strong velocity contrast at the 670-km discontinuity. The vanishing 410-km boundary may be attributed to the remnant of a subducted oceanic slab with increased Poisson's ratio in the transition zone.

Keywords Receiver functions · Inversion methods · Pannonian Basin · Crustal thickness · Shear wave

G. Hetényi (✉)
Laboratoire de Géologie, Ecole Normale Supérieure,
CNRS-UMR 8538,
24 rue Lhomond,
75005 Paris, France
e-mail: hetenyi@geologie.ens.fr

G. Hetényi
Department of Geophysics, Institute of Geography
and Earth Sciences, Eötvös Loránd University,
Pázmány Péter sétány 1/C,
1117 Budapest, Hungary

Z. Bus
Geodetical and Geophysical Research Institute,
Seismological Observatory,
Hungarian Academy of Sciences,
Meredek utca 18.,
1112 Budapest, Hungary

1 Introduction

The Pannonian Basin is the result of a Cenozoic kinematic history that began by the indentation of the Adrian microplate against the Alpine–Dinaric belt, followed by the extrusion of the Alcapa block to the NE (e.g., Tapponnier 1976; Horváth 1993; Bada et al. 2001). Seismic, seismological, and magnetotelluric studies show that the crust and lithosphere are thinned

beneath the entire basin (e.g., Ádám et al. 1989; Praus et al. 1990; Horváth 1993; Mónus 1995; Horváth et al. 2005; Grad et al. 2006), mainly due to the Miocene extension. Here, we perform a receiver function (RF) study using four permanent stations in Hungary to compare the crustal thickness to previous results obtained with other techniques and to determine crustal shear wave velocity structure. This study also extends results obtained with similar methods for neighboring regions in Central Europe (e.g., Wilde-Piórko et al. 2005; Heuer et al. 2007).

Teleseismic RFs are generally used to estimate the depth to the Moho and other seismic discontinuities. The technique is based on the delay time of generally P-to-S converted waves compared to the direct P wave (e.g., Langston 1979). Inversion of the RFs aims to determine the depth to the interfaces where the conversions occur, as well as the velocity model beneath the station. The principal problem is that the method yields relative velocities only, as the primary sensitivity of RFs is high wave-number velocity-changes and depth-velocity product (Ammon et al. 1990). To have better constraints on the absolute velocities, we perform two different types of inversions: a semilinearized and a stochastic one. Similar results may suggest that the obtained velocity model can be regarded in its absolute value.

RFs are also suitable to image upper mantle discontinuities. Using low-frequency data, we investigate the 410- and 670-km boundaries beneath the Pannonian Basin. The observed features are interpreted together with results from P wave tomography and refraction studies, and a hypothesis on the geodynamic evolution of the upper mantle is proposed.

2 RF calculation and analysis

We use the data of four permanent broadband STS-2 stations of the Hungarian Seismological Network located at different points of the Pannonian Basin: BUD in the north central, PKSM in the south central, PSZ in the northeastern, and SOP in the western part (Fig. 1). Although the basin is largely filled by a thick sedimentary cover, the stations are installed on exposed bedrock (dolomite, granite, andesite, and gneiss, respectively). Teleseismic data from between 30° and 95° epicentral distance and magnitudes above 5.5 were selected, and only low-noise traces with impulsive P wave arrival were kept. An attempt was made to select a few lower-magnitude events in back-azimuthal ranges containing no data. The acquisition period, the number of calculated RFs, as well as station coordinates are summarized in Table 1. The back-azimuthal distribution of the events is uneven with a majority of arrivals from the east, as most of the recorded earthquakes occurred in the area of the Japanese and Sumatran arcs.

RFs were calculated by the iterative deconvolution described in Ligorría and Ammon (1999). This method uses a series of Gaussian pulses (200 in this study) in the deconvolution of the vertical trace from

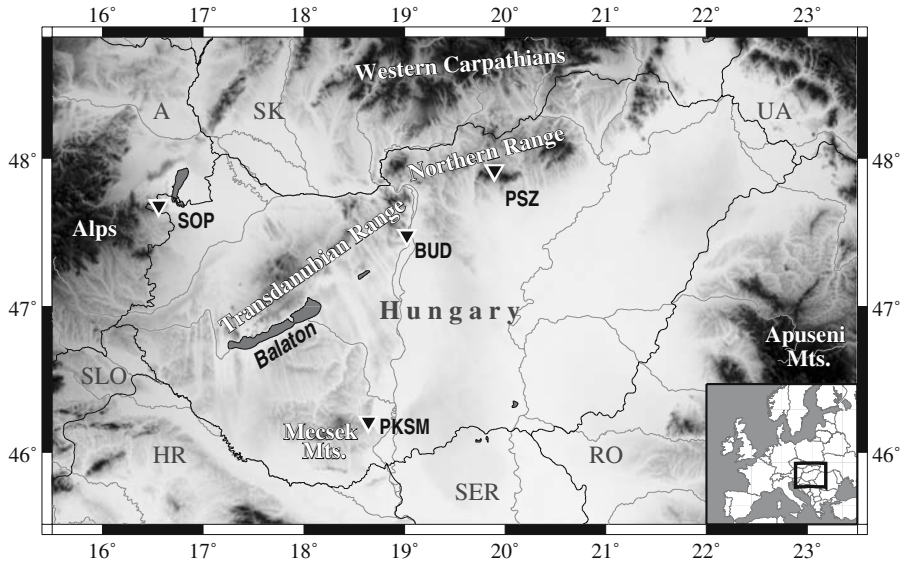

Fig. 1 Topographic map of Hungary and the surrounding region (see *inset* for the location within Europe), with the position of the four permanent broadband stations used in this study (*inverted triangles*). *White text* denotes major mountain ranges with exposed bedrock. Neighboring countries are Austria (*A*), Croatia (*HR*), Romania (*RO*), Serbia (*SER*), Slovakia (*SK*), Slovenia (*SLO*), and Ukraine (*UA*)

Table 1 A summary of station position, of data acquisition and quantity, as well as of main results

Station name	BUD	PKSM	PSZ	SOP
Latitude	47.4836°N	46.2119°N	47.9184°N	47.6833°N
Longitude	19.0239°E	18.6413°E	19.8944°E	16.5583°E
Altitude	196 m	170 m	940 m	260 m
Data collection period	1 year	1.5 years	10 years	1 year
Calculated traces	115	157	478	163
Selected traces	53	114	392	103
Grid search V_P/V_S	1.90	1.72	1.89	1.87
Moho depth (this study)	34 km	27 km	33 km	28 km
Moho depth (Horváth et al. 2005)	28 km	27 km	28 km	29 km

The average V_P/V_S is from the H–κ grid search method (Zhu and Kanamori 2000). See the text for the discussion on Moho depth results and comparison with previous values.

the radial and tangential ones. The width of the pulses, which controls the frequency content of the resulting RFs, was chosen to be equivalent to a 0.5-Hz low-pass filter. A second selection was then performed based on the amplitude and arrival time of the direct P wave after deconvolution; the number of selected RFs is shown in Table 1.

To minimize noise and to enhance coherent arrivals, the obtained radial and tangential RFs were stacked by 20°-wide back-azimuth ranges and are represented in Fig. 2 using a 10° overlap. The mean RF at each station is also represented on top, which was calculated by averaging the stacks of the back-azimuthal ranges. This prevents regions with numerous events to be overrepresented in the mean RF.

The main feature of the radial RFs is the P-to-S conversion of the Moho at between 3- and 4-s delay compared to the direct P wave arrival. Positive and negative multiples of this phase are also visible between 9- and 15-s delay. The variations of arrival time and amplitude with back-azimuth in the radial RF, together with the amplitude and polarity changes in the tangential RF, can be interpreted as effects of anisotropy and/or dipping boundaries beneath the stations (Savage 1998).

For example at station PSZ, the conversion from the Moho on the radial RF is at a constant delay time in the 180°–360° back-azimuth range, but shows an increasing arrival time between 0° and 180°. This temporal variation is accompanied by variations in the tangential RF, where the major polarity change has a 2π periodicity, which is indicative of a dipping interface. To estimate the dip of the Moho, we first calculated the aperture of the impinging waves beneath PSZ and picked the minimum and maximum arrival times of the P-to-S conversion. Then, using the obtained Moho depth and velocity structure (see the "Inversion results and discussion" section), we estimated the maximum dip of the crust–mantle boundary to be about 11° to the S–SW. The conversion at less than 1-s delay between 100° and 200° back-azimuth on the radial RF is related to the shallow structure of the Northern Range at station PSZ, the volcanic Mátra mountains, that have been tilted during Upper Miocene and Pliocene (Karátson et al. 2001). These interpretations are considered to explain the variations in arrival time of the RF; however, we later use the stacked RF to determine average Moho depth and crustal velocity beneath station PSZ.

In the case of BUD, there are no periodic variations in the RF, but three distinct domains can be delineated on the radial signal. Distinguishing upon the back-azimuth of the events, the signal corresponds to waves propagating and arriving from the Northern Range (between 0° and 40° back-azimuth), from the central Pannonian Basin (60°–120°), and from the Transdanubian Range (220°–280°). A better azimuthal coverage and more data would allow to confirm and to extend this interpretation.

The Moho conversion at PKSM and at SOP is at constant time delay, and the tangential RFs show small-amplitude signal only. However, at station SOP, the presence of a midcrustal conversion between 0° and 120° back-azimuth indicates that there may be differences in the velocity structure between the sedimentary basin lying to the northeast and the eastern termination of the Alps to the west.

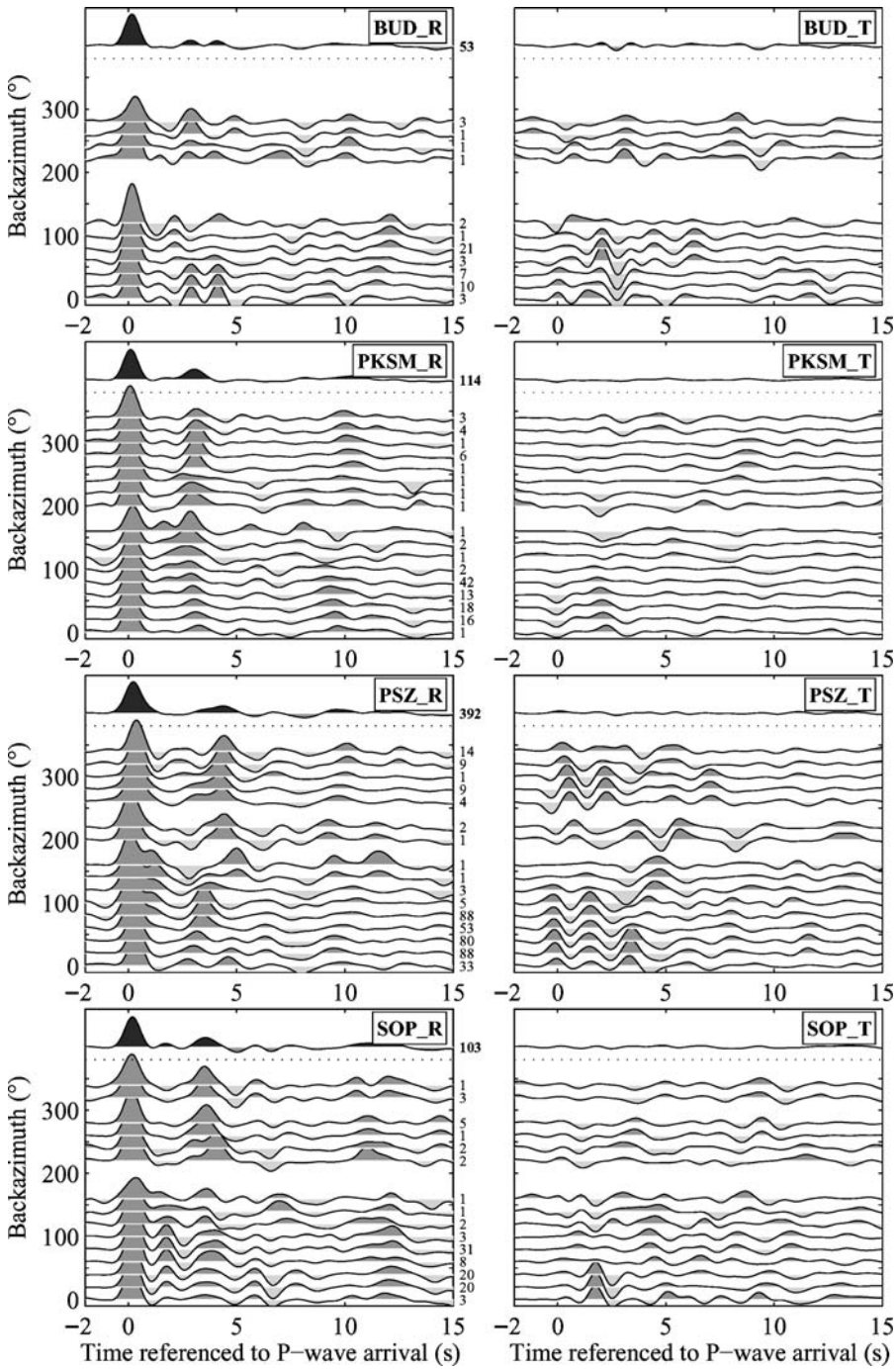

Fig. 2 RFs at each station and their variation by back-azimuth. *Left column*: radial component; *right column*: tangential component. Azimuthal stacks were calculated every 20° with a 10° overlap (*gray*). *Numbers on the right* show the number of traces in each stack (without overlap). The overall stack of back-azimuth ranges is shown on top of each figure (*black*)

3 Average V_P/V_S ratio determination

Taking advantage of the crust–mantle boundary's relatively clear P-to-S as well as multiple conversions, we determine the best-fitting Moho depth as well as average crustal V_P/V_S value by H–κ stacking (Zhu and Kanamori 2000). This method stacks the amplitude of the average RFs at the theoretical arrival times of the P-to-S and two multiple phases and searches over a parameter space of crustal thickness and average V_P/V_S. We use a weight of 0.4 for the P-to-S and a weight of 0.6 for both multiple phases along with an average crustal V_P of 6 km·s^{-1} (Mónus 1995). The obtained V_P/V_S ratios are shown in Table 1, and

the estimated error bar is about ±0.1. The V_P/V_S value falls into the average range at station PKSM; the slightly higher values can be explained by the composition of the crust underlying the other stations. These V_P/V_S values are used in the following part of the study where crustal thickness is constrained in two different ways.

4 Inversion methods

We perform RF inversions using two different methods to reveal Moho depth and the 1D crustal velocity structure. The mean RF for each station is represented in Fig. 2.

The first procedure is a semilinearized method by Ammon et al. (1990). It uses a finite number of thin layers of invariable thickness and searches for the best S wave velocity (V_S) structure that fits the RF observations. The major simplifications of this method are the following assumptions: the relationship between the data and the model is linear, and the V_P/V_S ratio of the crust is constant. Density is determined following Birch's Law (Birch 1961): $\rho = 0.32 \cdot V_P + 0.77$, where ρ is in g·cm^{-3} and V_P is in km·s^{-1}. To deal with the first simplification, we provide a range of 48 initial models during this inversion that are the perturbations of the average velocity model of the Pannonian Basin (Mónus 1995). As of the second assumption, we use the average V_P/V_S ratios derived above (Table 1). At the end of the inversion process, we keep 10 solutions with the lowest misfit based on least-squares misfit calculation.

The second inversion procedure is a stochastic method, the neighborhood algorithm (NA), described by Sambridge (1999). It is a direct search method to sample the parameter space: first, it chooses a number of initial parameter sets and calculates synthetic RFs. Then, with the use of an objective function, it ranks the tested models according to their misfit with the observed signal. The best n percent (80% in this study) is kept, and new parameter sets are tested in the neighborhood of the kept models. A large number of iterations guide the algorithm to preferentially sample the good data-fitting regions of the parameter space. During the application of the NA in this study, we use two (PKSM) or three (other stations) crustal layers overlying the mantle with a fixed velocity of V_P= 8 km·s^{-1} (Grad et al. 2006). The thickness, the V_P/V_S ratio, and the S wave velocity on top and at the bottom of each layer are allowed to vary between preset limits based on a priori data. During one inversion, 10,100 models are tested and ranked according to their misfit. According to Sambridge (2001), this is an acceptable number of models compared to the number of parameters, and a similar model/parameter ratio has provided accurate results on subsurface and crustal structure in other regions (Hetényi et al. 2006). Figure 3 shows the misfit of all tested models for the four stations. Based on a zoom on the best-ranked models, we keep and average the best 50 models for the discussion.

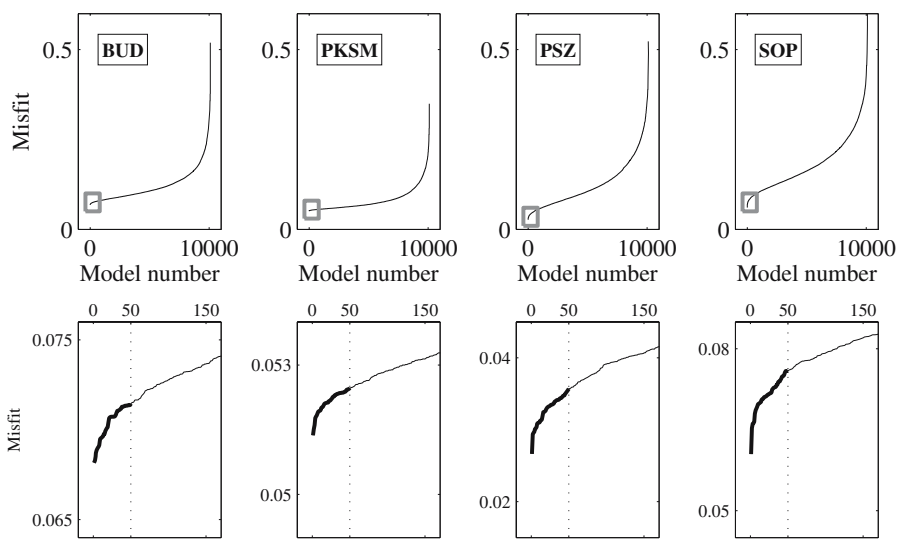

Fig. 3 Ranked misfit of the tested models for the NA inversion of the four RFs. *Top panels*: all models. *Bottom panels*: zoom on the area of the gray box on the top panel, showing the evolution of the misfit for the best-ranked models. For the discussion, the best 50 models (*thickened line*) were kept

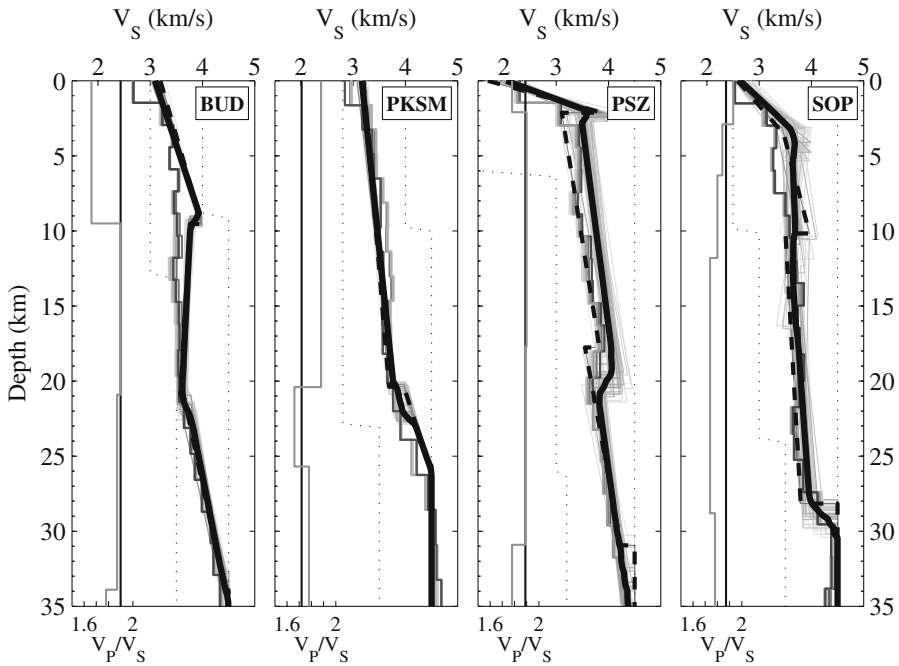

Fig. 4 Inverted S wave velocity models at the four stations. Step-like velocity models are the 10 best models from the constant V_P/V_S inversion (Ammon et al. 1990), with darker colors for better fitting RFs. Straight-line velocity models are the 50 best models from the NA-inversion (Sambridge 1999), using the same color code. The *thick black solid line* shows the average of the best 50 models, and the *thick black dashed line* the best fit model. *Dots* on both sides denote the imposed lower and upper limits for the NA inversion. The corresponding V_P/V_S ratios are shown on the *left side* of each panel: *black line* used in the constant V_P/V_S inversion, *gray line* obtained in the NA inversion

5 Inversion results and discussion

The results of the two inversion methods in terms of shear wave velocity at each station are represented in Fig. 4. Darker colors show better-fitting velocity models for both the semilinearized (step-like model) and the NA (straight segments) inversions. The best model is shown in thick dashed line, and the average of the best 50 results is shown in thick black line. V_P/V_S ratios obtained by the NA method are also represented, together with the constant V_P/V_S value computed above.

The main focus of the results is crustal thickness that we estimated based on the numerical value of the inversion results and their standard deviation. We also tried to define the Moho as the depth where P wave velocity exceeds 7.5 km·s^{-1}, or also as the midpoint of the higher velocity-gradient layer, the transition between the crust and the mantle. In all cases, these estimations agreed within 1–3 km.

Station BUD shows a crustal thickness of 34 km and an upper crust with a higher velocity gradient. The results of the two methods differ in the absolute value of the velocity in the upper crust, which is related to the different V_P/V_S ratios, but give similar results for the middle and lower crust.

The crust beneath PKSM has a uniform velocity gradient until about 20-km depth and has a 6- to 7-km-thick lower crust with a higher velocity gradient. The inversion methods result in very close velocity models and crustal thickness (27 km). Note that the best NA result is coincident with the average of the best 50 models both at stations BUD and PKSM.

The results obtained at PSZ are similar to those published by Bus (2003) using less data. There is a low surface velocity, high-gradient layer of about 3-km thickness, followed by a constant velocity gradient layer until 20-km depth. There is a clear velocity decrease between the upper and the lower crust, and the Moho is situated around 33-km depth. The V_P/V_S ratios in the two inversions are very similar. However, in the upper crust, there is a ±0.2 km·s^{-1} difference between the best NA, the average of the best 50 NA, and the semilinearized inversion results. This discrep-

ancy is probably related to the back-azimuthal variations discussed above.

Finally, with the exception of a higher velocity gradient layer close to the surface, most of the crust beneath SOP is of relatively constant velocity and nearly constant V_P/V_S. The jump at the Moho at 28 km is the sharpest among the four stations according to both inversion methods.

The obtained velocity profiles match well with the average velocity model of the Pannonian Basin (Mónus 1995). Comparison of the results from the two inversion methods shows that the velocity gradients obtained by the two types of inversion are equal, or at least very close. However, only in case of simple, relatively smoothly varying velocity profiles, the two methods give the same absolute velocities (e.g., PKSM or BUD lower crust). In other cases, such as in the upper crust beneath PSZ, the two velocity models may run in a parallel way and have a difference in their absolute values. These differences do not seem to correlate with the differences in the V_P/V_S ratio in the two models in all cases, and are probably inherent to the inversion methods.

Figure 5 compares the RFs obtained by inversion to the observations (bottom line) at each station. The traces have been shifted by two ticks along the vertical axis for better visibility. In general, the semilinearized inversion (middle lines) shows a better fit that is probably due to the assumed simplifications of the method and the use of numerous layers. The NA inversion gives results that are also very similar to the observations, especially at station PKSM. A larger spread among the best results of the semilinearized inversion at stations PSZ and SOP is visible both when comparing traces (Fig. 5) and the velocity models or Moho depth (Fig. 4).

We compare the obtained crustal thickness values to the ones presented in a recent compilation of available geophysical data (Horváth et al. 2005). Their crustal thickness map is mostly based on seismic measurements for petroleum exploration and a couple of active source refraction profiles that investigated lithospheric structure. Their observations of Moho depth are summarized in Table 1 and can be compared to our results.

There is an excellent match at stations PKSM and SOP, with a maximum difference of 1 km between seismic and RF results. Close to station SOP runs the CEL01 wide-angle reflection and refraction profile

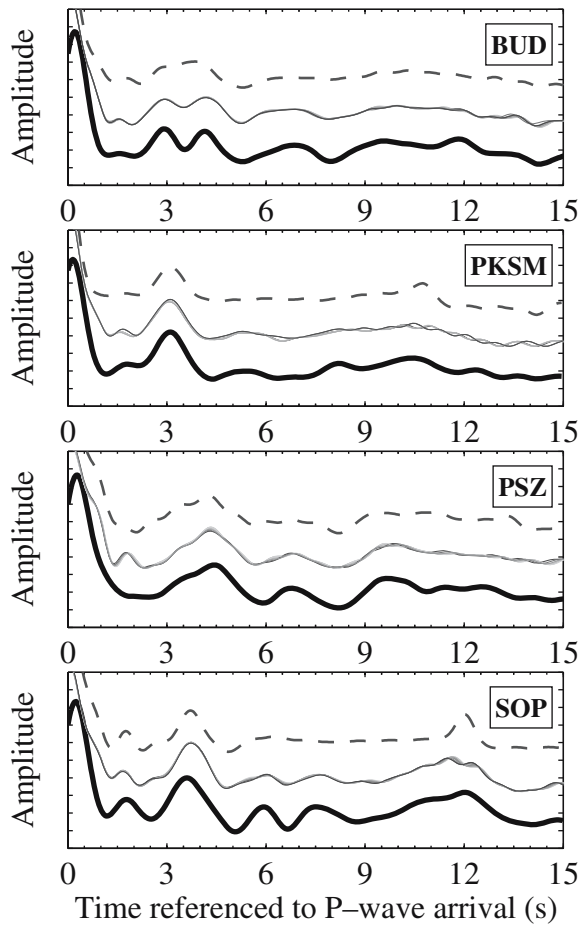

Fig. 5 Comparison of observed and inverted RFs at each station (shifted by two ticks on the vertical axis at each time, for better visibility): observed stacked trace (*bottom*, *thick black line*); the 10 best models from the constant V_P/V_S inversion (*middle*, *gray lines*); best model form the NA-inversion (*top*, *dashed line*)

(Środa et al. 2006): the observed Moho depth of 28–30 km is consistent with our results. Also, near station SOP is the eastern extent of the CEL09 refraction line (Hrubcová et al. 2005). According to their results, the velocity structure at the crust–mantle boundary is a broad gradient zone, but the used refraction line's extent is very limited in the Pannonian Basin, and the ray coverage is not representative. However, further northwest, the Moho depth of the Bohemian Massif is found to be at least 5 km deeper than our results at station SOP.

At stations BUD and PSZ, the differences between the RF study and the active seismic results compilation are about 5 km, the latter values being shallower.

Furthermore, the CEL05 line (Grad et al. 2006) shows a Moho at 25-km depth close to station PSZ, which is 8 km shallower than RF result. By taking into account the uncertainty of the RFs as well as those of the seismic profiles (about 1–2 km; Horváth, personal communication) and considering the fact that the velocity-transition zone at the Moho, probably about 3 km thick (Ligorría 2000), is seen from above by seismic experiments (sensitive to variations in V_P) and from below by RFs (sensitive to V_S), the results could be consistent. An easier explanation would be a minor correction of the map in Horváth et al. (2005). As the seismic profiles, by purpose, were located in the sedimentary areas of the basin and as their crustal thickness map is interpolated in other regions, including larger mountainous areas, drawing the 30-km Moho depth contour line all around the Transdanubian and Northern Range (and thus adding 2–5 km to crustal thickness) would be suitable. This is also supported by a coherent positive signal that follows the above ranges on the Bouguer anomaly map (Horváth et al. 2005).

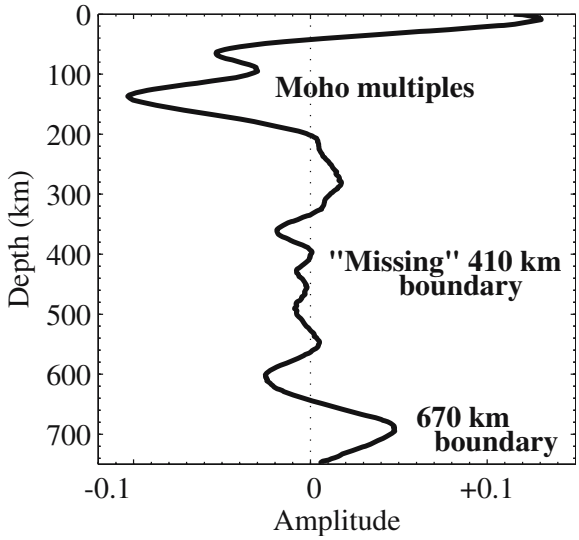

Fig. 6 Amplitude stack of low-frequency, migrated RFs with depth from all stations. The amplitude, related to relative changes in S wave velocity, clearly shows the presence of the 670-km boundary, but the 410-km boundary is missing. See text for further explication

6 Average upper mantle structure

The P-to-S converted waves are also used to image interfaces of the upper mantle. We calculated RFs at low frequency (equivalent to a 0.1-Hz low-pass filter) and performed a migration using the *iasp91* velocity model (Kennett and Engdahl 1991), including a move-out correction. As all piercing points are located within the Pannonian Basin, the obtained amplitudes with depth were then stacked into one vertical profile (Fig. 6) and are proportional to relative S wave velocity changes with depth. The peaks around 100 km depth are related to multiples of the Moho. The signature of the 670-km boundary is clear, but there is no sign of velocity jump at 410 km.

Świeczak et al. (2004) report from velocity models, constructed by fitting the measured and theoretical travel times of refracted and reflected phases of regional events having their bouncing points beneath SE Hungary, the two major upper mantle discontinuities to be at 420 and 670 km, respectively. Wortel and Spakman (2000) present several P wave tomography profiles in the Mediterranean–Carpathian region, showing a fast, cold anomaly that spans beneath the entire Pannonian Basin. The body extends vertically in between 410- and 670-km discontinuities, and its P wave anomaly is about +1.5%. The authors interpret that flat-lying anomaly at the bottom of the upper mantle as an entirely detached, subducted oceanic lithosphere.

The above references prove the existence of the upper mantle discontinuities seen by P waves. One viable solution to explain observations from RFs, sensitive to S waves, is a compositional variation of the zone between 410 and 670 km. Suppose that the flat-lying anomaly has an increased V_P/V_S ratio compared to the normal value, its V_S will be decreased, and thus, the jump in shear wave velocity with depth will be weakened at 410 km and enhanced at 670 km. Our calculations show that an increase of 0.1 in the value of the V_P/V_S ratio (corresponding to an increase of 0.02 in Poisson's ratio) would completely compensate the P wave anomaly and would entirely erase any change in V_S at 410 km. Other solutions to this problem may exist, but the fact that mafic rocks constituting the oceanic crust usually exhibit high V_P/V_S value is encouraging. Beside compositional variations, temperature also has a significant effect on velocity of the upper mantle, but a temperature anomaly of a given sign would

cause an anomaly of the opposite sign in both V_P and V_S (Cammarano et al. 2003). Also, the presence of lateral variations is possible but cannot be inferred with poor spatial coverage of a large area and unevenly distributed sources.

7 Conclusions

Comparison of two different inversion methods reveals that, in case of simple, smoothly varying velocity structures, they give very similar results that can be associated to absolute velocities. In more complicated cases, the methods give the same velocity gradient, but as expected, differ in their absolute values.

Application of the RF method at four stations in Hungary gives Moho depths between 27 and 34 km. The imaged crustal structure is coherent with the results of previous seismic and seismological investigations of the Pannonian Basin. We suggest that a minor correction should be brought to the thickness of the crust beneath the Transdanubian and Northern Ranges, modifying its value from less than 30 to more than 30 km. This modification also suggests the existence of local isostasy all along the mountainous region.

The deep structure revealed by RFs clearly shows the presence of the 670-km boundary. The absence of the 410-km boundary can be explained by increased V_P/V_S of the flat-lying, high-velocity anomaly beneath the Pannonian Basin, associated to the remnant of a subducted oceanic lithosphere.

Crustal thickness and velocity structure have been determined in four points of the basin only. Longer data collection periods will provide better azimuthal coverage and more robust inversions to investigate both shallow, crustal structure, and upper mantle discontinuities as well. Future studies should include permanent stations from other countries in the basin, joint inversion with surface waves and tomography, and experiments with more densely spaced arrays to achieve better constraints and to image lateral variations.

Acknowledgment We are grateful to Jérôme Vergne for providing helpful hints about receiver functions and to Frank Horváth for the discussion on the geodynamics of the Pannonian Basin. We acknowledge the anonymous reviewers for their constructive comments which improved the manuscript and associate editor Jiří Zahradník for his assistance. The seismological data are from the GFZ Seismological Data Archive (http://www.gfz-potsdam.de/geofon/). The map figure was produced with GMT (Wessel and Smith 1991). We thank Charles J. Ammon and Malcolm Sambridge for making publicly available their receiver function analysis and NA inversion tools, respectively, which were used in this study.

References

Ádám A, Landy K, Nagy Z (1989) New evidence for the distribution of the electric conductivity in the Earth's crust and upper mantle in the Pannonian Basin as a "hotspot". Tectonophysics 164:361–368

Ammon CJ, Randall GE, Zandt G (1990) On the nonuniqueness of receiver function inversions. J Geophys Res 95:15303–15318

Bada G, Horváth F, Cloething S, Coblentz D, Tóth T (2001) Role of topography-induced gravitational stresses in basin inversion: the case study of the Pannonian Basin. Tectonics 20(3):343–363

Birch F (1961) The velocity of compressional waves in rocks to 10 kilobars, part 2. J Geophys Res 66:2199–2224

Bus Z (2003) S-wave velocity structure beneath the Mátra Mountains (Hungary) inferred from teleseismic receiver functions. Acta Geod Geophys Hung 38(1):93–102

Cammarano F, Goes S, Vacher P, Giardini D (2003) Inferring upper-mantle temperatures from seismic velocities. Phys Earth Planet Inter 138(3):197–222

Grad M, Guterch A, Keller GR, Janik T, Hegedűs E, Vozár J, Ślączka A, Tiira T, Yliniemi J (2006) Lithospheric structure beneath trans-Carpathian transect from Precambrian platform to Pannonian Basin: CELEBRATION 2000 seismic profile CEL05. J Geophys Res 111:B03301

Hetényi G, Cattin R, Vergne J, Nábělek JL (2006) The effective elastic thickness of the India Plate from receiver function imaging, gravity anomalies and thermomechanical modelling. Geophys J Int 167(3):1106–1118

Heuer B, Kämpf H, Kind R, Geissler WH (2007) Seismic evidence for whole lithosphere separation between Saxothuringian and Moldanubian tectonic units in central Europe. Geophys Res Lett 34:L09304

Horváth F (1993) Towards a mechanical model for the formation of the Pannonian Basin. Tectonophysics 226:333–357

Horváth F, Bada G, Windhoffer G, Csontos L, Dövényi P, Fodor L, Grenerczy G, Síkhegyi F, Szafián P, Székely B, Timár G, Tóth L, Tóth T (2005) Atlas of the present-day geodynamics of the Pannonian Basin: Euroconform maps with explanatory text. http://geophysics.elte.hu/projektek/geodinamikai_atlasz_eng.htm

Hrubcová P, Środa P, Špičák A, Guterch A, Grad M, Keller GR, Brueckl E, Thybo H (2005) Crustal and uppermost mantle structure of the Bohemian Massif based on CELEBRATION 2000 data. J Geophys Res 110:B11305

Karátson D, Csontos L, Harangi Sz, Székely B, Kovácsvölgyi S (2001) Volcanic successions and the role of destructional events in the Western Mátra Mountains, Hungary:

implications for the volcanic structure. Géomorphologie 2:79–92

Kennett BLN, Engdahl ER (1991) Traveltimes for global earthquake location and phase identification. Geophys J Int 105:429–465

Langston C (1979) Structure under Mount Rainier, Washington, inferred from teleseismic body waves. J Geophys Res 84:4749–4762

Ligorría J, Ammon CJ (1999) Iterative deconvolution and receiver-function estimation. Bull Seismol Soc Am 88:1395–1400

Ligorría JP (2000) An investigation of the mantle–crust transition beneath North-America and Poisson's ratio of the North American Crust. Ph.D. thesis, Saint Louis University – St. Louis, MO, USA

Mónus P (1995) Travel time curves and crustal velocity model for the Pannonian basin. Technical Report, MTA GGKI, Budapest, 6 pp

Praus O, Pěčová J, Petr V, Babuška V, Plomerová J (1990) Magnetotelluric and seismological determination of the lithosphere-asthenosphere transition in Central Europe. Phys Earth Planet Inter 60:212–228

Sambridge M (1999) Geophysical inversion with a neighbourhood algorithm – I. Searching the parameter space. Geophys J Int 138:479–494

Sambridge M (2001) Finding acceptable models in nonlinear inverse problems using a neighbourhood algorithm. Inverse Problems 17:387–403

Savage MK (1998) Lower crustal anisotropy or dipping boundaries? Effects on receiver functions and a case study in New Zealand. J Geophys Res 103:15069–15087

Środa P, Czuba W, Grad M, Guterch A, Tokarski AK, Janik T, Rauch M, Keller GR, Hegedüs E, Vozár J, CELEBRATION 2000 Working Group (2006) Crustal and upper mantle structure of the Western Carpathians from CELEBRATION 2000 profiles CEL01 and CEL04: seismic models and geological implications. Geophys J Int 167(2):737–760

Świeczak M, Grad M, TOR and SVEKALAPKO working groups (2004) Upper mantle seismic discontinuities topography variations beneath Eastern Europe. Acta Geophys Pol 52(3):251–270

Tapponnier P (1976) Évolution tectonique du système alpin en Méditerranée: poinçonnement et écrasement rigide-plastique. Bull Soc Géol France XIX(3):437–460

Wessel P, Smith WHF (1991) Free software helps map and display data. EoS Trans. AGU, 72, pp. 441 and 445–446

Wilde-Piórko M, Saul J, Grad M (2005) Differences in the crustal and uppermost mantle structure of the Bohemian Massif from teleseismic receiver functions. Stud Geophys Geod 49(1):85–107

Wortel MJT, Spakman W (2000) Subduction and slab detachment in the Mediterranean–Carpathian region. Science 290:1910–1917

Zhu L, Kanamori H (2000) Moho depth variation in southern California from teleseismic receiver functions. J Geophys Res 105:2969–2980